Monograph:

Billings, S.A., Tsang, K.M. and Tomlinson, G.R. (1987) Application of the NARMAX Method to Nonlinear Frequency Response Estimation. Research Report. Acse Report 319 . Dept of Automatic Control and System Engineering. University of Sheffield

Application of the NARMAX Method to Nonlinear Frequency Response Estimation

by

S A Billings*
K M Tsang*
G R Tomlinson†

*Department of Control Engineering
University of Sheffield, Sheffield

†Department of Mechanical Engineering
Heriot-Watt University, Edinburgh

Research Report No 319

October 1987

6th. International Modal Analysis Conference, 1-4 Feb 1988 Hyatt Orlando USA

APPLICATION OF THE NARMAX METHOD TO NONLINEAR FREQUENCY RESPONSE ESTIMATION

S A Billings*, K M Tsang* and G R Tomlinson†

*Department of Control Engineering
University of Sheffield
Sheffield, UK

†Department of Mechanical Engineering
Heriot-Watt University
Edinburgh, UK

ABSTRACT

The NARMAX method of identifying the frequency domain characteristics of nonlinear systems is illustrated by computing the first, second and third order generalised frequency response functions of a heat exchanger.

NOMENCLATURE

d	time delay
f_s	sampling frequency
α	constant
β	parameter vector
T	sampling interval
$\varepsilon(k)$	prediction errors
$u(k)$	input
$y(k)$	output
$\xi(k)$	residuals
$H_i(-)$	generalised frequency response functions

INTRODUCTION

The identification of the frequency domain characteristics of nonlinear systems is of fundamental importance in many branches of science and engineering. Although several authors(1) have considered the theoretical analysis of such ideas only a few researchers have attempted to produce estimates of the generalised frequency response functions from measured signals of real processes of unknown model structure. In the few cases where such results have been attempted only the first and second order functions were estimated on the assumption that all higher order terms were zero. In the present study a parametric estimation method based on the NARMAX (Nonlinear AutoRegressive Moving Average model with eXogenous inputs) model is described. By considering the identification of a nonlinear heat exchanger it is shown that the method can provide estimates of the generalised frequency response functions of any order and the first, second and third order functions are estimated and analysed.

THE NARMAX METHOD

A wide class of nonlinear systems can be represented by the NARMAX model(2)

$$y(t) = \alpha+F^{\ell}\big[y(t-1),\dots y(t-n_y),u(t-d),\dots u(t-d-n_u+1),\varepsilon(t-1),\dots\varepsilon(t-n_\varepsilon)\big]+\varepsilon(t) \qquad (1)$$

where $u(t)$ and $y(t)$ represent the measured input and output respectively. $\varepsilon(t)$ is the prediction error

$$\varepsilon(t) = y(t)-\hat{y}(t)$$

n_u, n_y, n_ε represent the number of lags in the input, output and prediction error, d is the time delay, α a constant, and $F^{\ell}(\cdot)$ is some nonlinear function of degree ℓ. The Volterra, bilinear and other well known nonlinear models can be shown to be special cases of eqn (1). In the present analysis $F^{\ell}(\cdot)$ will be expanded as a polynomial although other choices such as rational functions etc can be made.

A NARMAX model with first order dynamics expanded as a second order polynomial nonlinearity would for example be represented as

$$x(k) = C_1x(k-1)+C_2u(k-1)+C_{11}x^2(k-1)+C_{12}x(k-1)u(k-1)+C_{22}u^2(k-1) \qquad (2)$$

If the output is measured with additive noise

$$y(k) = x(k)+e(k)$$

the NARMAX model becomes

$$y(k) = C_1y(k-1)+C_2u(k-1)+C_{11}y^2(k-1)+C_{12}y(k-1)u(k-1)+C_{22}u^2(k-1)+e(k)-C_1e(k-1)-2C_{11}y(k-1)e(k-1)+C_{11}e^2(k-1)-C_{12}e(k-1)u(k-1) \qquad (3)$$

and cross-product noise terms appear in the expansion. In general the noise may enter the system internally and because the system is nonlinear it will not always be possible to translate it to be additive at the output. Any nonlinear identification procedure should therefore take account of this phenomena. Unfortunately, most of the parameter estimation algorithms developed for linear systems cannot be applied to equation (3) because even though the model is linear-in-the-parameters the noise is not independent of the input. Notice that only a small number of parameters are required to describe the system eqn (3) by a NARMAX model whereas the Volterra series expansion of this system would require thousands of terms to characterize the system using $h_1(\cdot)$, $h_2(\cdot,\cdot)$, $h_3(\cdot,\cdot,\cdot)$ etc[3]. Because the NARMAX model utilizes the information in the past output measurements it has a much smaller parameter set than the functional series expansions. Although it was derived from a totally different approach the NARMAX model can be visualised as a Volterra series in the inputs and outputs.

Several parameter estimation algorithms have been derived for the NARMAX model. Most of these algorithms are based upon defining the following vectors associated with the model of eqn (3) for example,

$$x_k^T = [y(k-1), u(k-1), y^2(k-1), y(k-1)u(k-1), u^2(k-1), \varepsilon(k-1), \varepsilon(k-1)y(k-1), u(k-1)\varepsilon(k-1), \varepsilon^2(k-1)]$$

$$\hat{\beta}^T = [\hat{c}_1, \hat{c}_2, \ldots \hat{c}_s]$$

$$\varepsilon(k+1) = y(k+1) - x_{k+1}^T\hat{\beta} \quad (4)$$

With these definitions several parameter estimation algorithms can be utilized to estimate $\hat{\beta}$. Although it may be tempting to model the system as a series of threshold piecewise linear models this will often yield results that are biased and virtually useless for prediction[5]. It is important therefore to be able to estimate the parameter vector β in models such as eqn (3) and (4) and one way to achieve this is to derive a prediction error algorithm based on minimising the cost function

$$J_2(\beta) = \frac{1}{N} \log_e \det \sum_{k=1}^{N} \varepsilon(k;\beta)\varepsilon^T(k;\beta) \quad (5)$$

Notice, however, that the determination of the model structure or which terms to include in the NARMAX model expansion is vitally important[4],[5]. Consequently, all the parameter estimation algorithms derived for the NARMAX have incorporated a structure detection module. A new orthogonal estimation algorithm derived for the NARMAX model provides an alternative solution to this problem[7]. The algorithm allows each coefficient in the model to be estimated independently of the other terms in the model because of the orthogonality property which holds for any input and shows the contribution that each term makes to the output. The results of a new updated version of this algorithm will be described below.

Whichever model formulation or identification procedure is implemented it is important to test that the identified model does adequately describe the data set. This will be true providing the following simple tests are satisfied[4],[6]

$$\phi_{\xi\xi}(\tau) = \delta(\tau) \qquad \phi_{u\xi}(\tau) = 0 \;\forall\, \tau$$

$$\phi_{u^{2\prime}\xi}(\tau) = 0 \;\forall\, \tau \qquad \phi_{u^{2\prime}\xi^2}(\tau) = 0 \;\forall\, \tau \quad (6)$$

$$\phi_{\xi\xi u}(\tau) = 0 \;\forall\, \tau \geq 0$$

Once the NARMAX model coefficients have been estimated and the model validated the generalized frequency response functions

$$H_n(\omega_1, \omega_2 \ldots \omega_n) = \int_{-\infty}^{\infty}\!\!\ldots\int h_n(\tau_1, \tau_2 \ldots \tau_n) \exp\{-j(\omega_1\tau_1 + \ldots \omega_n\tau_n)\} d\tau_1 \ldots d\tau_n \quad (7)$$

can be computed using the probing or harmonic input method[8],[9]. To compute $H_1(j\omega_1)$ for example set $u(k) = e^{j\omega kT}$, $y(k) = H_1(j\omega)e^{j\omega kT}$ in the NARMAX model and equate terms of $e^{j\omega kT}$. To compute the second order function set $u(k) = e^{j\omega_1 kT} + e^{j\omega_2 kT}$, $y(k) = H_1(j\omega_1)e^{j\omega_1 kT} + H_1(j\omega_2)e^{j\omega_2 kT} + 2!\, H_2(j\omega_1, j\omega_2) e^{j(\omega_1+\omega_2)kT}$ and equate coefficients of $2!e^{j(\omega_1+\omega_2)kT}$ to yield $H_2(j\omega_1, j\omega_2)$. Similarly for the higher order generalized frequency response functions $H_3(j\omega_1, j\omega_2, j\omega_3)$, $H_4(j\omega_1, j\omega_2, j\omega_3, j\omega_4)$ etc.

PARAMETRIC SPECTRAL ESTIMATES OF A HEAT EXCHANGER

A complete description of the heat exchanger system, the experiment design, data collection and earlier nonlinear model fitting is available in the literature[10]. In the present analysis the identification of the nonlinear frequency response characteristics will be computed by re-estimating a NARMAX model based on the latest versions of our parameter estimation algorithms.

Throughout the data will consist of 500 data pairs from an experiment with an input bandwidth of 0.5Hz augmented with 500 data pairs from a separate experiment with input bandwidth 0.05Hz. The output data is illustrated in Fig.1. Only the first 500 data pairs will be used to fit the models, the second 500 data pairs from an independent experiment with a different input will be used to test the prediction accuracy of the model. This is a severe test for any model fitting algorithm but is we believe particularly important when fitting models, linear or nonlinear, to data generated from a nonlinear system[4],[6]. All the data were obtained by sampling the real signals at 0.3 secs and in all the experiments a mean level was added to the input.

Initially, the simple nonlinear detection test $\phi_{y'y'^2}(\tau)$[4] was applied to the output data (recorded in response to an input with dc shift and third order moments zero) to determine if the system was linear or nonlinear. The results illustrated in Fig.2 clearly show that $\phi_{y'y'^2}(\tau)$, is well outside the 95% confidence limits indicating that the system under test is highly nonlinear. Despite this result it is of interest to fit a linear model to the data initially.

The forward regression orthogonal algorithm (this is a recent extension of the orthogonal estimator) produced the following model structure and estimates after ten iterations

$$y(k) = -0.186+1.772y(k-1)+0.273u(k-1)-0.751y(k-2)$$
$$-0.298u(k-2)+\varepsilon(k)-0.1\varepsilon(k-1)-0.028\varepsilon(k-2)$$
$$+0.22\varepsilon(k-3)-0.16\varepsilon(k-4)-0.17\varepsilon(k-5) \qquad (8)$$

The model validity tests, eqn (6), for this model and a comparison of the system output and predicted output of the model are illustrated in Figs.3 and 4 respectively. In Fig.3 $\phi_{u^{2'}\xi}(\tau)$ and $\phi_{u^{2'}\xi^2}(\tau)$ are outside the confidence bands indicating that the model will be biased because nonlinear terms have been omitted. From Fig.4 however the model appears to predict the output well for points 400-500 but is clearly deficient over points 500-750. This is to be expected because the model was estimated using points 0-500 only. Forcing the model to predict over data from a separate experiment (points 500-1000) however clearly shows it is biased. An optimised model computed using a prediction error routine[6] produced a model with almost identical deficiencies.

Previous experience[6] has shown that linear modelling often provides a reasonably good starting estimate of the orders of n_u, n_y, n_ε and d to select in eqn (1). On this basis therefore the forward regression orthogonal algorithm was given the initial specification $n_y = 2$, $n_u = 2$, $n_\varepsilon = 5$, $d = 1$, degree of polynomial expansion $\ell = 3$ and produced the following model after ten iterations

$$y(k) = 2.035+0.924y(k-1)+0.452u(k-1)-0.0163y^2(k-1)$$
$$-0.00065u(k-2)y(k-1)u(k-1)-0.00194y^2(k-1)$$
$$u(k-1)-0.0018u^3(k-1)-0.0083u^2(k-1)+\varepsilon(k)$$
$$-0.037\varepsilon(k-1)-0.029\varepsilon(k-2)+0.21\varepsilon(k-3)$$
$$+0.076\varepsilon(k-4)-0.15\varepsilon(k-5) \qquad (9)$$

Note that from the 220 possible terms that could have been included in the above model the algorithm has deleted the vast majority of these because they were found to be insignificant. The structure detection algorithm which decides which terms to include in the final model usually performs extremely efficiently. It is however important to check that the structure is correct and the parameters unbiased and to modify or add to the model as appropriate[6],[10]. These objectives are easily achieved by checking the model validity tests eqn (6) and the prediction accuracy of the fitted model which for the model above are illustrated in Figs.5 and 6 respectively.

The model validity tests Fig.5 are now acceptable and confirm that the model eqn (9) is a good fit to the data. Inspection of the predicted output of the nonlinear model eqn (9) illustrated in Fig.6 clearly shows that the model produces good predictions over both the data used in estimation (points 0-500) and over data from an independent experiment (points 500-1000) and even predicts the saturation just after point 500. A comparison of the predicted output of the linear model Fig.4 with the predicted output of the nonlinear model Fig.6 demonstrates the superior performance of the latter.

Using a prediction error algorithm based on the structure of eqn (9) produced the model

$$y(k) = 2.036+0.924y(k-1)+0.45u(k-1)-0.0163y^2(k-1)$$
$$-0.00063u(k-2)y(k-1)u(k-1)-0.0019y^2(k-1)u(k-1)$$
$$-0.00183u^3(k-1)-0.0085u^2(k-1)+\varepsilon(k)-0.037\varepsilon(k-1)$$
$$-0.0269\varepsilon(k-2)+0.20\varepsilon(k-3)+0.067\varepsilon(k-4)$$
$$-0.15\varepsilon(k-5) \qquad (10)$$

A comparison of the two models in eqn's (9) and (10) shows that they are virtually identical. The fact that two different estimation algorithms give the same results gives further confidence in the model. The results above also compare well with the model estimated using an earlier stepwise regression/prediction error algorithm[10].

The generalised frequency response functions of any order can now be computed by applying the probing method described earlier to the estimated model in eqn (10). The probing method is applied by ignoring the $\varepsilon(\cdot)$ or prediction error terms since these represent a model of the noise and were included in the model to ensure the process model parameter estimates are unbiased. The first order generalised transfer function is illustrated in Fig.7 and shows the system has a low pass type characteristic. Fig.8 which shows the linear output, first and second harmonic superimposed on one plot indicates that the harmonics are very significant at low frequencies. All the frequency response plots are against normalised frequency. Multiplying the normalised frequency by the sampling frequency gives hertz. A normalised frequency of 0.5 (equivalent to $f_s/2$ say) therefore corresponds to the highest frequency which can be seen in $H_1(\cdot)$ when the original data was sampled at a normalised frequency of 1.0 (equivalent to f_s). Following a similar argument the results for $H_2(j\omega_1, j\omega_2)|\omega_1 = \omega_2$ and $H_3(j\omega_1, j\omega_2, j\omega_3)|\omega_1 = \omega_2 = \omega_3$ in Fig.8 are only relevant for normalised frequencies less than 0.25 and 0.166 (equivalent to $f_s/4$, $f_s/6$) respectively.

The second order frequency response function $H_2(j\omega_1, j\omega_2)$ is illustrated in Fig.9a with the corresponding contour plot in Fig.9b. These plots are dominated by the intermodulation effects represented by the ridge along $f_1+f_2 = 0$, and the strong peak for f_1 and f_2 close to zero. These properties[11] indicate that for low frequencies $H_2(\cdot,\cdot)$ will induce nonlinear distortion and a dc shift in the output.

The third order frequency response function $H_3(j\omega_1, j\omega_2, j\omega_3)$ is illustrated in Fig.10a with the corresponding contour plot in Fig.10b. Both Fig. 10a and 10b display $H_3(f_1,f_2,f_3)$ for $f_3 = f_1$; alternatively f_3 can be fixed if required. Using Fig.10b to interpret the results the peak at A shows that for f_1,f_2 close to zero a strong intermodulation effect will be produced. There is a strong ridge along $f_1+f_2 = 0$ (ie $f_1+f_2+f_3 = f_1-f_1+f_1 = f_1$), B in the diagram, indicating a significant compression effect. The ridge denoted by C along $2f_1+f_2 = 0$ (ie $f_1+f_2+f_3 = f_1-2f_1+f_1 = 0$) suggests the system will produce a significant dc shift in the output. The ridge tagged D along $f_1+f_2 = 0.5$ should be ignored since it is outside the relevant frequency band for $H_3(\cdot,\cdot,\cdot)$ (see the discussion for Fig.8 above).

In a similar manner $H_4(-),H_5(-),H_6(-)$ etc can be readily computed directly from the estimated NARMAX model eqn (10), the only problem is how to display the results.

The above interpretation of the estimated higher order frequency response functions can be confirmed and analysed by injecting inputs into the NARMAX model eqn (10) corresponding to areas of interest identified in $H_1(\cdot),H_2(-)$ and $H_3(-)$. For example simulating the estimated NARMAX model eqn (10) (set $\varepsilon(k) = 0\ \forall k$) for a sinusoidal input of normalised frequency 0.01 produced the results illustrated in Fig.11. The constant term 2.036 in eqn (10) has been subtracted from the outputs in order to show the strong dc shift produced by the nonlinearities of the system. Inspection of Fig. 11 shows that as predicted there is a strong dc shift in the system output (due to the ridge $f_1+f_2 = 0$ in $H_2(-)$ and $2f_1+f_2 = 0$ in $H_3(-)$ etc) and the output is distorted. The model response for any other input can be obtained in exactly the same way, and this allows the experimenter to predict the response of the system under test to any input, not just the input used to estimate the model. Such an approach is extremely difficult to achieve if an FFT based algorithm is used to estimate $H_1(-),H_2(-)$ etc.

CONCLUSIONS

The NARMAX method of estimating the generalised frequency response functions of nonlinear systems has been illustrated by analysing data from a heat exchanger. The results represent just one example of the type of analysis which can be achieved using this approach. The NARMAX method has several advantages compared with other FFT based algorithms; $H_i(-)$ can be computed for all i, the results are not input dependent and work for sensible record lengths (ie a few hundred data points), many properties of $H_i(-)$ can be determined and once identified the model can be simulated in the time or frequency domain to show the response to any input.

ACKNOWLEDGEMENTS

The authors (SAB and GRT) gratefully acknowledge financial support for the work presented above from SERC, ref GR/D/75809.

REFERENCES

(1) Brillinger, D.R., Rosenblatt, M.: Asymptotic theory of estimates of k'th order spectra; in B. Harris (Ed): Spectral Analysis of Time Series; Wiley 1967.

(2) Leontaritis, I.J., Billings, S.A.: Input-output parametric models for nonlinear systems, Part I - Deterministic nonlinear systems, Part II - Stochastic nonlinear systems; Int. J.Control, 41, 303-344, 1985.

(3) Billings, S.A.: Identification of nonlinear systems; in Billings, S.A., Gray, J.O., Owens, D.H. (Eds): Nonlinear System Design; P. Peregrinus, 1985.

(4) Billings, S.A.: Introduction to nonlinear systems analysis and identification; in Godfrey, K., Jones, P. (Eds): Signal Processing for Control; Springer, 1986.

(5) Billings, S.A., Voon, W.S.F.: Piecewise linear identification of nonlinear systems; Int.J.Control, 1987, 46, 215-235.

(6) Billings, S.A., Voon, W.S.F.: A prediction error and stepwise regression estimation algorithm for nonlinear systems; Int.J. Control, 44, 803-822, 1986.

(7) Billings, S.A., Korenberg, M.J., Chen, S.: Identification of nonlinear output-affine systems using an orthogonal least squares algorithm; (in press).

(8) Gifford, S.J., Tomlinson, G.R.: A functional series approach in the identification of nonlinear structures; 5th IMAC, London, 1987.

(9) Billings, S.A., Tsang, K.M.: Estimating higher order spectra; 5th IMAC, London, 1987.

(10) Billings, S.A., Fadzil, M.B.: The practical identification of systems with nonlinearities; 7th IFAC Symp. Ident. and Syst. Par. Est., 155-160, 1985.

(11) Vinh, T., Chouychai, T., Liu, H., Djouder, M.: Second order transfer function computation and physical interpretation; 5th IMAC, London, 1987.

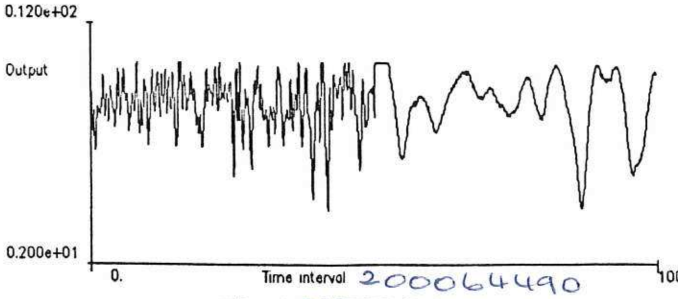

Fig.1 System output

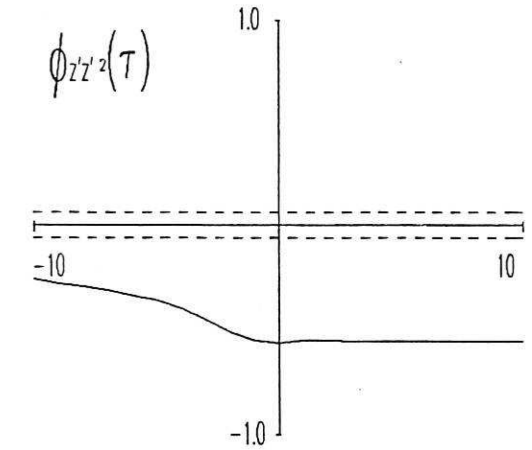

Fig.2 $\phi_{y'y'^2}(\tau)$ Test

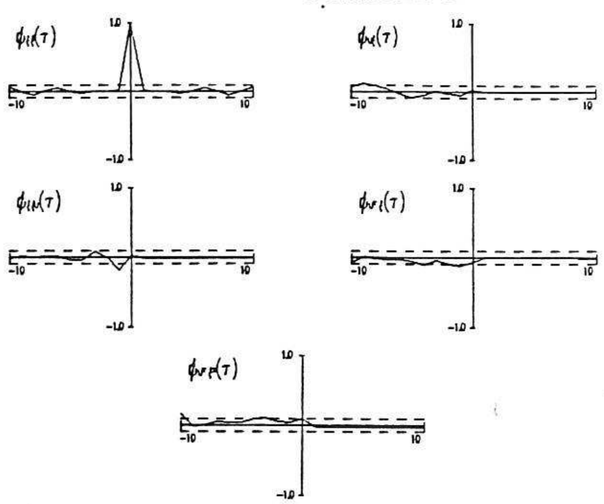

Fig.5 Model validation - nonlinear model

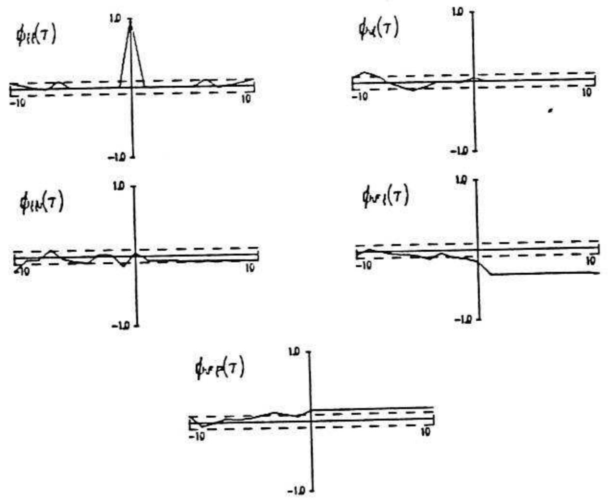

Fig.3 Model Validation - linear model

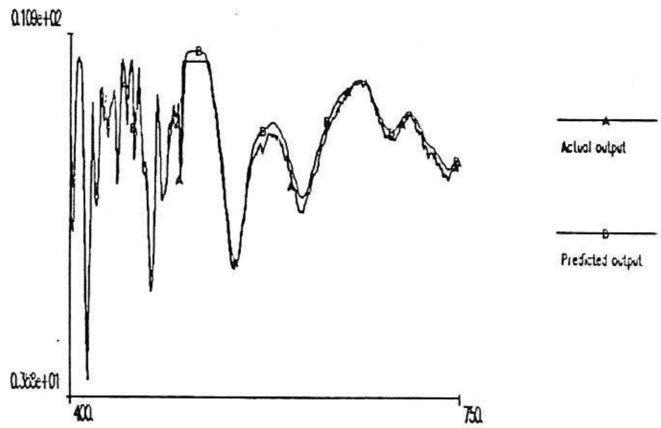

Fig.6 Prediction - nonlinear model

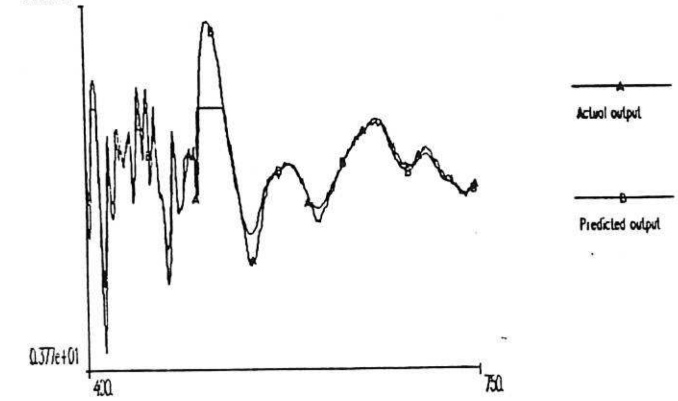

Fig.4 Prediction - linear model

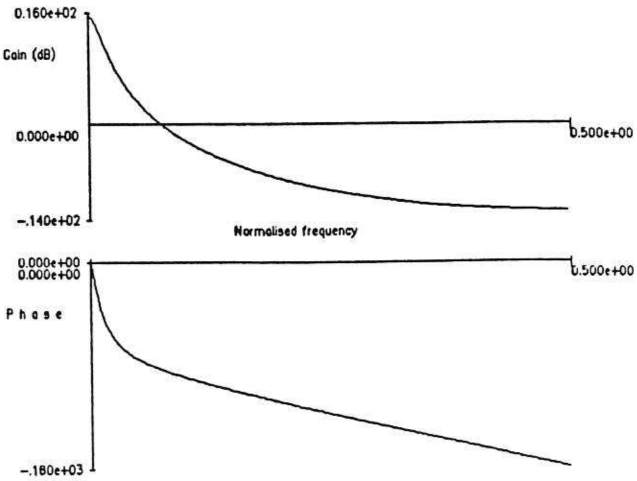

Fig.7 $H_1(j\omega)$

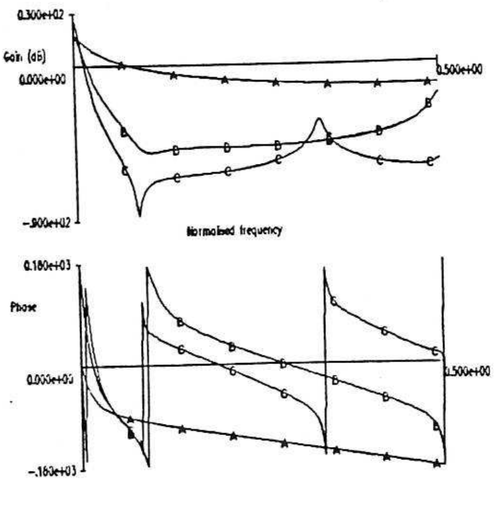

Fig.8 Harmonic plot

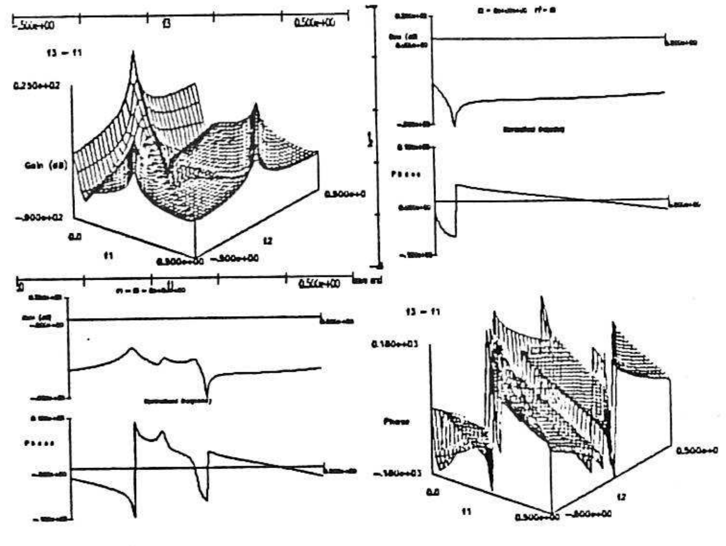

Fig.10a $H_3(j\omega_1,j\omega_2,j\omega_3)$

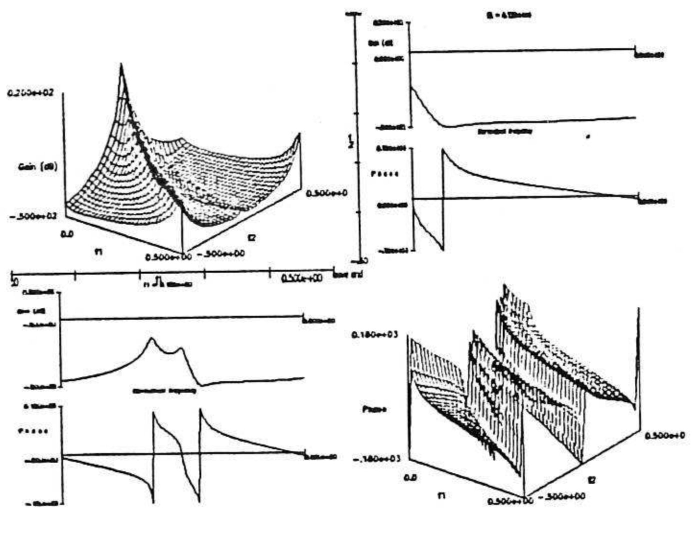

Fig.9a $H_2(j\omega_1,j\omega_2)$

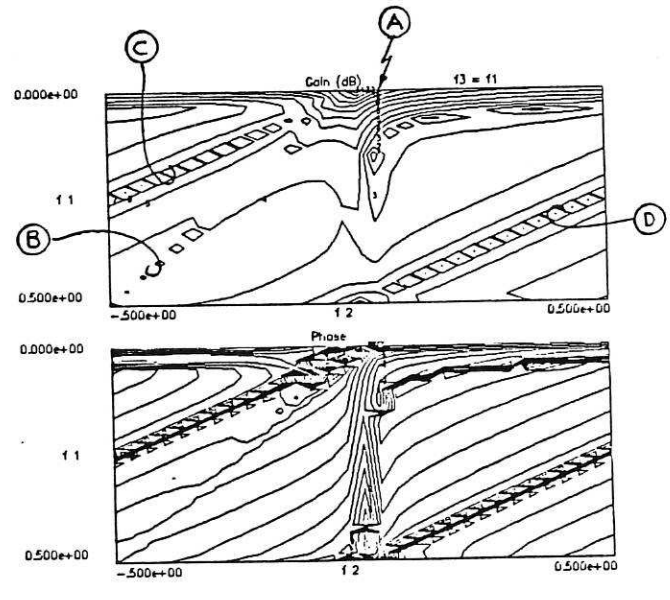

Fig.10b $H_3(j\omega_1,j\omega_2,j\omega_3)$ - contour plot

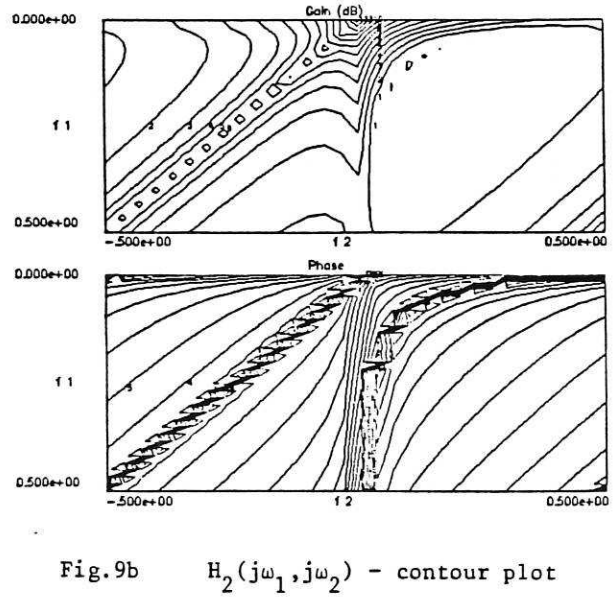

Fig.9b $H_2(j\omega_1,j\omega_2)$ - contour plot

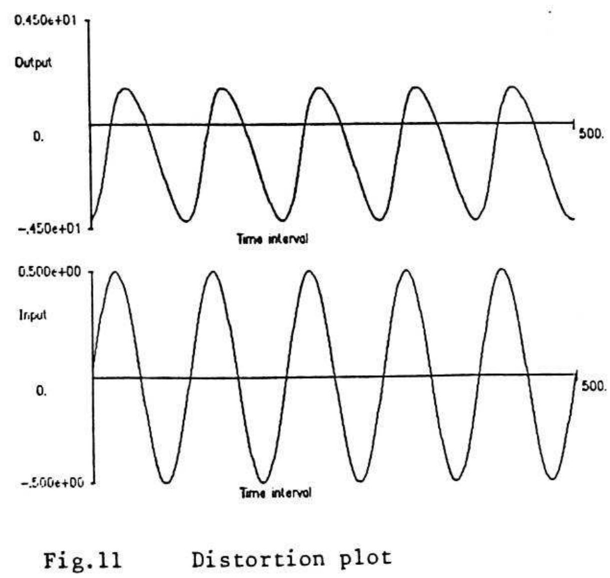

Fig.11 Distortion plot